Fluorescence lifetime fluctuations of single molecules probe the local environment of oligomers around the glass transition temperature

R. A. L. Vallée,[a] M. Baruah, J. Hofkens, F. C. De Schryver, N. Boens, and M. Van der Auweraer
Department of Chemistry and Institute of Nanoscale Physics and Chemistry (INPAC), Katholieke Universiteit Leuven, 3001 Heverlee, Belgium

D. Beljonne
Laboratory for Chemistry of Novel Materials, University of Mons-Hainaut, Place du Parc 20, 7000 Mons, Belgium

(Received 8 November 2006; accepted 20 March 2007; published online 10 May 2007)

Single molecule fluorescence experiments have been performed on a BODIPY-based dye embedded in oligo(styrene) matrices to probe the density fluctuations and the relaxation dynamics of chain segments surrounding the dye molecules. The time-dependent fluorescence lifetime of the BODIPY probe was recorded as an observable for the local density fluctuations. At room temperature, the mean fraction of holes surrounding the probes is shown to be unaffected by the molecular weight in the glassy state. In contrast, the free volume increases significantly in the supercooled regime. These observations are discussed in the framework of the entropic theories of the glass transition. © *2007 American Institute of Physics*. [DOI: 10.1063/1.2728902]

I. INTRODUCTION

Understanding the cause for the slowing down of the dynamics of supercooled liquids and the occurrence of the resulting glass transition to an amorphous solid is one of the main challenges of condensed matter physics.[1–6] The various theories that have been put forward to explain the phenomenon have been broadly classified into two categories. Thermodynamic ones describe the observed glass transition as a kinetically controlled manifestation of an underlying quasi-equilibrium phase transition between the supercooled metastable fluid and an ideal metastable glass phase.[3,6] Both entropy and free volume theories pertain to this category.[3] According to the nonthermodynamic (kinetic) viewpoint, best represented by the mode coupling theory,[2] vitrification occurs as a result of a purely dynamic transition from an ergodic to a nonergodic behavior.[2,3,6] Although recent experimental evidences of spatially heterogeneous dynamics in glass-forming liquids have led to a further understanding of the origin of the slowing-down mechanism,[7–9] no consensus has been reached as to which scenario better describes the glass transition.

Because it allows bypassing the ensemble averaging intrinsic to bulk studies, single molecule spectroscopy (SMS) constitutes a powerful tool to assess the dynamics of heterogeneous materials at the nanoscale level.[10–13] Using two-dimensional (2D) orientation techniques, the in-plane (of the sample) projection of the transition dipole moment of the single molecule (SM) [the so-called linear dichroism $d(t)$] has been followed in time, and its time correlation function $C_d(t)$ has been computed and fitted by a stretched exponential function $f(t)=e^{-(t/\tau)^{\beta}}$.[14–17] These investigations have allowed identifying static and dynamic heterogeneity in the samples,[8,9] i.e., SMs exhibit τ and β values varying according to (i) their actual position in the matrix and (ii) the time scale at which they are probed as a result of the presence of different nanoscale environments. More recently, the full three-dimensional (3D) orientation of the emission transition dipole moment of a SM has been recorded as a function of time.[18–22] In particular, the distribution of nanoscale barriers to rotational motion has been assessed by means of SM measurements[23] and related to the spatial heterogeneity and nanoscopic α-relaxation dynamics deep within the glassy state. Owing to the high barriers found in the deep glassy state, only few SMs were able to reorient, while somewhat lower barriers could be overcome when increasing the temperature. In another context, we have shown that the fluorescence lifetime of single molecules with quantum yield close to unity is highly sensitive to changes in local density occurring in a polymer matrix.[24–29] Using free volume theories, we have related the lifetime fluctuations to hole (free volume) distributions and have determined the number of polymer segments involved in a rearrangement cell around the probe molecule as a function of temperature,[24,27] solvent content,[25] and film thickness.[26] Based on a microscopic model for the fluctuations of the local field,[28] we have established a clear correlation between the fluorescence lifetime distributions measured for single molecules and the local fraction of surrounding holes.

In this paper, we extend our investigations to the behavior of a newly synthesized bifluoroborondipyrromethene (BODIPY) probe embedded in various molecular weight M_n oligo(styrene) (OS) matrices. Indeed, the glass transition temperature T_g depends on the degree of polymerization of the chain (N), according to the Fox-Flory empirical equation $T_g(\infty)-T_g(N)\propto 1/N$.[30] The free volume approach provides a

[a]Electronic mail: renaud.vallee@chem.kuleuven.be

theoretical foundation to the Fox-Flory equation, which rests on the assumption that chain ends contribute an excess free volume. A decrease in N leads to an increase of chain end concentration and thus an increase in free volume. This increase in free volume should, in turn, lead to a decrease in T_g. Experimental investigations[31] have led to the conclusion that the Fox-Flory equation is not valid anymore at very low molecular weights. The Gibbs and Di Marzio entropy theory[32] was found to better describe $T_g(N)$, especially for short chains.[31] The lattice model of Gibbs and Di Marzio is a minimal model for polymers that accounts for chain stiffness and the variation of volume with temperature. It predicts the occurrence of an ideal thermodynamic second-order glass transition, with vanishing configurational entropy, occurring at a temperature T_2 which is about 50 K below T_g. According to this theory, and in contrast to the free volume concept, the number of holes present in the matrix below T_2 is constant.[32] Our SMS experimental approach based on fluorescence lifetime fluctuations[24–29] provides a direct access to the fraction of holes surrounding the probe molecule in the considered polymer matrix and thus appears as a particularly relevant technique able to discriminate between these two theories. At room temperature, we observe that the mean fraction of holes surrounding the probes is independent of the molecular weight of the polymer in the glassy state. In contrast, it increases significantly in the supercooled regime. These observations clearly support the interpretation formulated by Gibbs and Di Marzio.

The paper is organized in the following way: (i) We first show that we have really measured single molecules by checking the outcome of antibunching experiments (Sec. III A). (ii) We determine the typical time scale on which the lifetime fluctuations occur by use of a minimal binning approach in the analysis of the successive photon arrival time lags between excitation and emission (Sec. III B). (iii) We describe the observed fluorescence lifetime fluctuations on the time scale determined in (ii) and give evidence for the importance of the use of the proper time scale in order to observe the fluctuations (Sec. III C). (iv) We (re)describe the local field microscopic theory that allows us to determine the local fraction of holes surrounding the probe molecule on the basis of their lifetime fluctuations (Sec. III D) and provide the actual values determined by a comparison between theory and experiment (Sec. III E). (v) We provide clear evidence that the lifetime fluctuations cannot be due to reorientations of the SMs close to the polymer film-air interface, reinforcing our interpretation in terms of a fluctuating density of the local surrounding in the bulk (Sec. III F). We finish with our conclusions.

II. MATERIALS AND METHODS

The BODIPY probe [Fig. 1(a)] (4,4- difluoro-8-(4-methoxyphenyl)-3-[-2-(4-methoxyphenyl)ethenyl]- 1,5,7-trimethyl-3a,4a-diaza-4-bora-s-indacene) used in this study has been designed specifically to fulfill the following criteria: (i) it is highly photostable; (ii) it has a luminescence quantum yield close to 1 (0.99 in toluene) such that the observed fluorescence lifetime has a largely dominant radiative part;

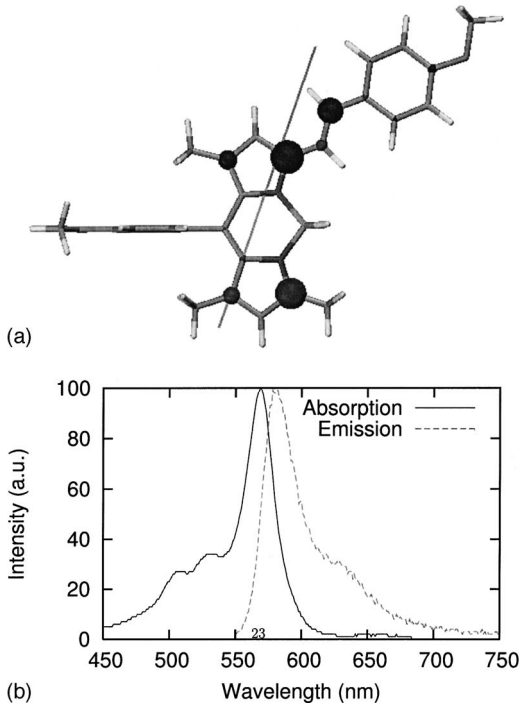

FIG. 1. 2D schematic structure of the BODIPY probe synthesized specifically for the present study. The arrow describes the orientation of the emission transition dipole moment of the molecule ($|\boldsymbol{\mu}|=11.4$ De); the atomic transition densities are also displayed (Ref. 25) (b) Steady state absorption and emission spectra of the probe molecule dissolved in toluene at $10^{-6}M$.

(iii) it emits in the red part of the visible spectrum [emission maximum at 584 nm, Fig. 1(b)], hence minimizing overlap with the autofluorescence of the matrix; and (iv) it is structurally rigid.

Samples were prepared by spin-coating a dilute solution of the probe ($10^{-10}M$) and oligo(styrene) (OS) in toluene onto a glass substrate. Annealing was performed in order to remove the solvent and relax the stresses induced by the deposition procedure. The films obtained this way had a thickness of $\approx$100 nm. Eight samples were prepared, each sample consisting of highly monodisperse OS chains (Polymer Source, polydispersity index ranging from 1.06 to 1.10, $M_n=1860$, 2000, 2500, 3700, 4700, and 7500 and Polymer Standard Service, $M_n=662,869$), in order to perform the experiments below and above T_g while keeping the temperature fixed at $T=292$ K. The glass transition temperatures (T_g) of the OS compounds were determined by the use of a differential scanning calorimeter (DSC) (822e, equipped with an intracooler, Mettler Toledo).

The single molecule experiments were performed with an inverted confocal scanning optical microscope (Olympus IX70). The excitation light, i.e., pulses of 1.2 ps at a repetition rate of 8 MHz (Spectra Physics, Tsunami, OPO, Pulse Picker and Doubler) and a wavelength $\lambda=568$ nm [Fig. 1(b)], was circularly polarized and the power set to 1.1 μW at the entrance port of the microscope. In order to eliminate any residual excitation signal in the fluorescence emission, a suitable combination of filters was used, consisting of a bandpass (BP568, Chroma) placed in the excitation path, a dichroic (Olympus 570), a notch (Kaiser Optics, 568) that matches the bandpass, and a long pass (LP580, Chroma) in

the emission path. The time lags between excitation and emission were measured by use of an avalanche photodiode (SPCM-AQ-14, EG & G Electro Optics) equipped with a time-correlated single photon counting (TCSPC) card (Becker & Hickl GmbH, SPC 630) used in the first in first out (FIFO) mode. A suitable window of 18.4 ns (time width of 72 ps per channel for the 256 channels available in the FIFO mode) was chosen to adequately build the decay profiles. In order to observe the dynamics (lifetime transients) of single molecules in a polymer matrix, short bin sizes have to be taken (100 ms, see below). The decay profiles built on such a time scale count 500–10 000 photons. The maximum likelihood estimation (MLE) method that is known to give stable results even at total counts less than 1000 (Ref. 33) was used to fit these profiles. In the antibunching experiment, the fluorescence signal from individual BODIPY molecules was split by a 50/50 nonpolarizing beam splitter and led towards two avalanche photodiodes, delayed by 1.47 μs, according to the classical Hanbury-Brown and Twiss coincidence experiment.[34] The delay time between consecutive photons was acquired using the TCSPC card mentioned above. Histograms of the interphoton times (coincidences) were built. Given the pulsed excitation, coincidences in the histogram accumulate at nT (n integer), where T is the time between two consecutive pulses (125 ns).

The quantum-chemical calculations were performed using the following methodology. Ground-state optimizations were performed at the semiempirical Hartree-Fock Austin Model 1 (AM1) level[35] and excited-state optimizations by coupling the AM1 Hamiltonian to a full configuration interaction (CI) scheme within a limited active space, as implemented in the AMPAC package.[36] The optical absorption and emission spectra were then computed by means of the semiempirical Hartree-Fock intermediate neglect of differential overlap (INDO) method, as parametrized by Zerner *et al.*,[37] combined to a single configuration interaction (SCI) technique; the CI active space is built here by promoting one electron from one of the highest 60 occupied to one of the lowest 60 unoccupied levels.

The Monte Carlo simulations, allowing us to calculate the radiative lifetime of a dye molecule embedded in a disordered medium, were performed using a homemade software.[28] In these simulations, the spectroscopic properties (transition dipole moment, transition energy, polarizability) of the BODIPY probe determined by quantum-chemical calculations were used. To model the effect of the environment on the probe molecule, the polarizability of a monomer of poly(styrene) was also determined.

III. RESULTS

A. Coincidence measurement

A sophisticated method that allows one to insure the probing of single molecules consists in performing an antibunching (or coincidence) measurement.[38–43] Photon antibunching is a clear signature of a nonclassical radiation field, which reflects the fact that a single quantum system cannot spontaneously emit two photons at the same time, without cycling back to its excited state. Photon antibunching has been measured for individual molecules by measuring the interphoton arrival times.

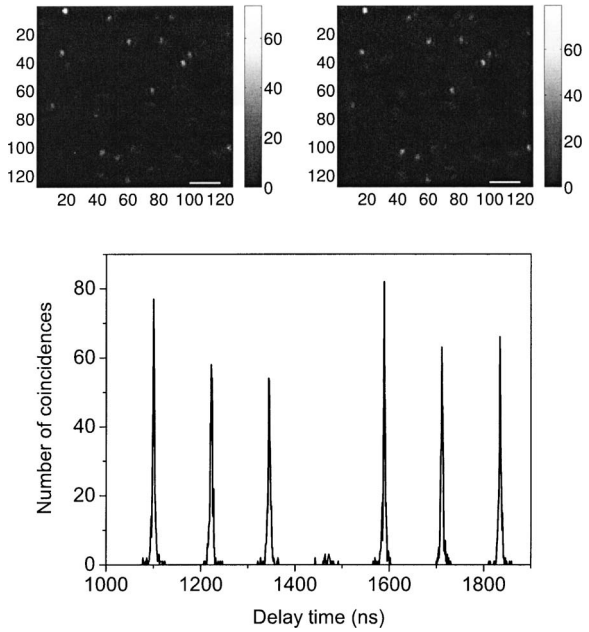

FIG. 2. (Top) 10×10 μm^2 (128×128 pixels) areas of the sample scanned at a rate of 500 Hz/pixel in order to localize the molecules. Two channels delayed by 1.47 μs were used in this case to perform an antibunching experiment. (Bottom) The coincidence measurement shows that two photons are not simultaneously emitted by the same spot (intensity close to zero at the time corresponding to the delay introduced between the two channels). The chosen molecule is the bright upper left one in the scan plots. The interdistance between the successive peaks in this graph corresponds to the inverse repetition rate of the laser, set to 8 MHz.

Figure 2 (top) shows two 10×10 μm^2 areas, scanned at a rate of 500 Hz/pixel and obtained by collecting the signals from two avalanche photodiodes delayed one with respect to the other by 1.47 μs, of an OS sample (M_n=7500) containing the probe molecules. The number of molecules observed in each frame is the one expected for the concentration of probe molecules incorporated in the OS matrix. Neither blinking nor photobleaching behavior is observed on these frames, which confirms the characteristic features of the probe molecule (very high quantum yield and high photostability). Remarkably, the probe molecule has an average fluorescence rate of 40 000 counts/s with peaks as high as 70 000 counts/s for the upper left very bright molecule, at the set excitation power, which makes this substance a very good choice for SMS measurements. A coincidence measurement performed on the bright upper left molecule is shown in Fig. 2 (down). Clearly, at the delay time corresponding to the delay introduced between the two channels, no coincident photons occur. Peaks of coincidence only appear at discrete steps nT (n integer), where T=125 ns is the time between repeated pulsed excitations. The full width at half maximum of these peaks gives an estimation of the fluorescence lifetime of the observed dye ($\approx$3.5 ns). These observations performed on a few dye molecules insure that we are indeed recording the fluorescence emission of single monochromophoric systems, which is essential in achieving our goal of probing the nanosurrounding of a single dye in a polymer matrix.

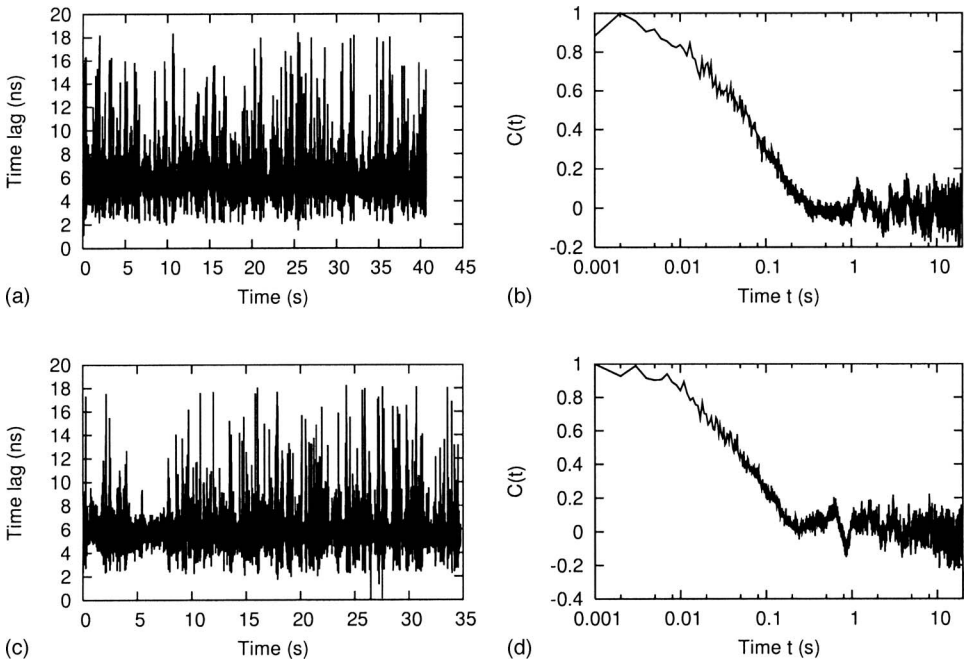

FIG. 3. Trajectories of decay times obtained via a minimal binning approach (see text for details), for the probe molecule (molecule 1) embedded in an OS matrix with M_n=662 during the first 40 s (a) and the following 35 s time range (c). [(b) and (d)] Corresponding autocorrelation functions.

B. Minimal binning approach

According to previously reported studies,[24–29] the fluorescence lifetime of a single molecule embedded in a polymer matrix exhibits (strong) fluctuations. In order to determine the time scale on which these fluctuations occur, we performed a minimal binning analysis[13,45] of the arrival time lags between excitation and spontaneously emitted photons in the case of a single dye molecule embedded in the OS matrix that is expected to show the highest mobility, i.e., the OS matrix with M_n=662, T_g=272 K. Following this methodology, the single molecule time trajectory is discretized with a time increment $\Delta_{\max}$ such that there is at least one photon in each chronological bin. The value of $\Delta_{\max}$ is simply dictated by the value of the maximum difference in the chronological time between consecutive detected photons in the selected part of the whole trace. In each chronological bin, the decay time τ_b is then defined as the arithmetic mean of the time lags $\tau(t)$ between excitation and fluorescence photons for the number of photons n_b detected in this bin: $\tau_b=\Sigma\tau(t)/n_b$.

Figure 3 shows two subtraces [(a) and (c)] of the decay time of the recorded transient of a dye (specific dye molecule followed in this study, referred to as molecule 1) embedded in a M_n=662 OS matrix, obtained with the minimal binning approach. For each of the traces, $\Delta_{\max}$ has been determined to be very close to 1 ms, so that, for the sake of simplicity, we just apply the minimal binning analysis with $\Delta_{\max}$ =1 ms. The corresponding autocorrelation functions of τ_b are shown in Figs. 3(b) and 3(d). In both cases, the autocorrelation functions decay with a relaxation time ζ of about 100 ms. Owing to the facts that the binning time $\Delta_{\max}$ =1 ms (i.e., much shorter than the determined correlation time) and the chosen subtraces last for about 40 s (i.e., much longer than the determined decay time), the decays and thus the values obtained for the mean relaxation time ζ $\approx$100 ms are statistically reliable.[44]

C. Observation of fluorescence lifetime fluctuations

The reference fluorescence lifetime of the molecules dissolved in a toluene solution is 3.44 ns as determined by TCSPC. Figure 4 shows the decay profiles obtained by accumulating all photons falling in a bin time of 100 ms, comparable to the relaxation time ζ. The three decay profiles correspond to three subtraces extracted from the trajectory of molecule 1, i.e., a molecule embedded in an OS matrix with M_n=662, during the first 20 s of its recording [Fig. 3(a)]. Very interestingly, on this binning time scale of 100 ms, the three decay profiles show large variations of the decay time. All three decays were best fitted by single exponential functions, with fluorescence lifetimes τ=3.21, 3.65, and 5.15 ns.

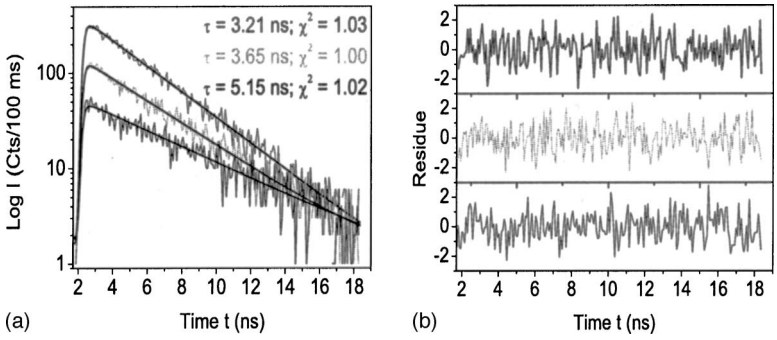

FIG. 4. Decay profiles (a) recorded (during 100 ms) at different times during the measurement of molecule 1. Also shown are the best fits obtained by MLE fitting of the profile together with the plot of the weighted residuals (b) and the values of the χ^2 criterion used in the MLE fit. All data were best fitted by single exponential functions. The estimated lifetimes are indicated.

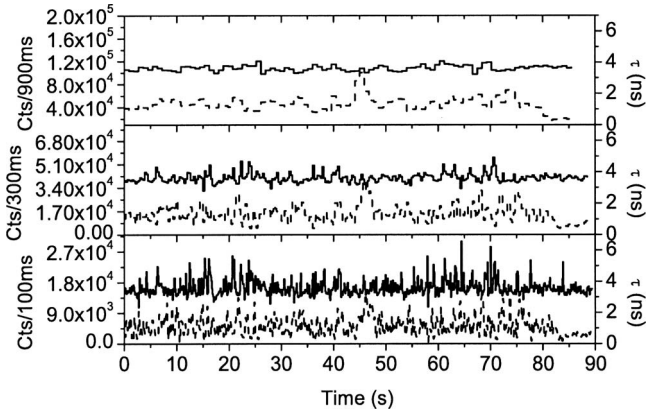

FIG. 5. Fluorescence intensity (dash) and lifetime (solid) trajectories of molecule 1, with all photons grouped in successive bins of 100, 300, 900 ms from bottom to top, respectively. The contribution of statistical noise in the determination of the lifetime is negligible for the number of counts considered in these traces [see also Fig. 8(a)] (Ref. 33).

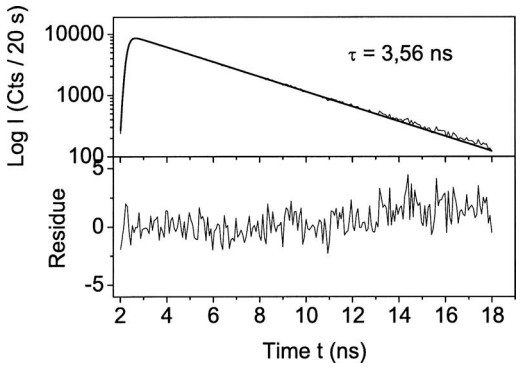

FIG. 6. Decay profile (top) recorded during the first 20 s of the measurement of molecule 1 in the OS matrix with M_w=662. Also shown are the best fit obtained by MLE fitting of the profile and the plot of the weighted residuals (bottom). The profile was fitted by a single exponential function with τ=3.56 ns (Ref. 48).

Performing a binning on the time scale ζ of the relaxation process taking place in the matrix, as observed in the minimal binning analysis, thus allows one to observe strong fluctuations of the fluorescence lifetime. As reported elsewhere,[24–29] these fluctuations of the probe fluorescence lifetime reflect local density fluctuations of the surrounding polymer matrix. The basic explanation for the observed behavior is the following: after pulsed photoexcitation, the probe relaxes to its ground state by spontaneous emission of a photon. The electric field associated with this photon (electric field generated by the transition dipole moment of the molecule) polarizes and thus induces dipole moments $\boldsymbol{\mu}_k$ on the surrounding OS monomer units. The observed emission consequently originates from an effective transition dipole moment $\boldsymbol{\mu}_{\text{tot}}$, which is the sum of the molecular emission transition dipole moment (source dipole) $\boldsymbol{\mu}$ and of the dipoles $\boldsymbol{\mu}_k$ induced in the medium surrounding the probe,

$$\boldsymbol{\mu}_{\text{tot}} = \boldsymbol{\mu} + \sum_k \boldsymbol{\mu}_k. \tag{1}$$

The measured radiative lifetime $\tau \infty |\boldsymbol{\mu}|^2/|\boldsymbol{\mu}_{\text{tot}}|^2$ of the probe (quantum yield very close to 1) thus crucially depends on the positions and polarizabilities of the dye and the surrounding OS monomers.

We want to point out that the time scale chosen to bin the photons is a very critical parameter. Figure 5 (bottom) shows the intensity and fluorescence lifetime trajectories of molecule 1 built by binning the photons on the 100 ms time scale. Strong fluctuations of the lifetime are observed as a result of the expected strong fluctuations of the positions of the styrene units surrounding the probe in the polymer melt. However, if the chosen binning time is too large, an intrinsic averaging effect takes place, which smooths out the whole trace. Figure 5 (from bottom to top) shows such traces, where the binning time has been set to 100, 300, and 900 ms.

These figures clearly evidence smearing out of the fluorescence lifetime fluctuations as the binning time scale is increased. The physical effect behind these observations is simply that the monomers surrounding the probe have had time to spatially rearrange their position many times so that, on these longer binning time scales, only an average polarization effect is observed. It is worth noticing that the decay times reported in Fig. 5 (top and middle) still are true fluorescence lifetimes, as in each case the decay profiles obtained were best fitted by monoexponential functions. As a further proof of this averaging effect, we built a decay profile by accumulating all the photons recorded during the first 20 s of the observation of molecule 1. This decay profile, shown in Fig. 6, is still fitted by a monoexponential function with a fluorescence lifetime τ=3.56 ns.[48]

In order to observe fluorescence lifetime fluctuations, special care has thus to be taken in the choice of the binning time of the photons, which must be lower or equal to the intrinsic time scale for the local motion of the monomers. Of course, this time scale depends on the mobility of the polymer matrix, and thus on the difference $T-T_g$ (T=292 K being the temperature at which the experiment is performed). By choosing a binning time of 100 ms, i.e., approximately equal to the relaxation time ζ determined in the most mobile matrix, we make sure to observe the lifetime fluctuations in all other matrices (being more supercooled or in the glassy state), which have a longer relaxation time scale.

D. Fluorescence lifetime fluctuations: Theory

The fluorescence lifetime fluctuations of the BODIPY probe reflect the local density fluctuations of the surrounding matrix. In particular, the time scale for these fluctuations reflect the time scale for the segmental rearrangements and thus the mobility of the investigated matrix. Based on a macroscopic approach,[24,27] we have indeed related the fluorescence lifetime fluctuations to an effective dielectric constant (defined as a spatially averaged quantity on a length scale comparable to the transition wavelength), varying from position to position in the matrix and depending on the local fraction of holes surrounding directly the SM in the matrix. This way, we could determine the number of polymer segments involved in a rearrangement cell around the probe molecule as a function of temperature,[24,27] solvent content,[25] and film thickness.[26] More recently, we have developed a microscopic model[28] generalizing the Lorentz approach to local field effects. Owing to this model,[28] we have estab-

lished a clear correlation between the fluorescence lifetime distributions measured for SMs and the local fraction of surrounding holes. We have further validated this model in investigating the specific interaction of SMs with the surrounding polymer chains.[29] For the sake of completeness, we outline briefly here below the main steps involved in the simulations of this microscopic model, which allows us to assess the simulated lifetime distributions of the system under investigation.

(i) We used the Hartree-Fock semiempirical AM1 technique to assess the geometric and electronic structures of the BODIPY molecule in both the S_0 singlet ground state and the S_1 lowest singlet excited state. Frequency calculations were performed to validate the existence of the recovered local minima. The excited-state properties of the molecule were determined by INDO/SCI calculations on the basis of the AM1 excited-state geometries. The transition dipole moment $|\boldsymbol{\mu}|=3.8\times10^{-29}$ *SI* and the polarizability $\chi=5.7\times10^{-39}$ *SI* were estimated for the probe molecule. Similar calculations performed for the styrene unit lead to a polarizabilty $\alpha=1.0\times10^{-39}$ *SI*.

(ii) The probe molecule is represented by an ensemble of atomic transition densities [Fig. 1(a)] and displays a polarizability χ. The probe is located at the origin of a 3D cubic lattice and surrounded by z polarizable monomers of polarizability α. To mimic the motion of the styrene units around the fixed probe molecule, a given fraction of holes (with zero polarizability) is introduced in the lattice. To determine the lattice constant Δ, the van der Waals volume of a styrene unit $V=1.19\times10^{-28}$ m^3 is simply attributed to the volume $V=\Delta^3$ of a cell in the cubic lattice. To calculate the effective transition dipole of the probe, we have solved the system of coupled linear equations

$$\boldsymbol{\mu}_k=\alpha_k\left[\mathbf{E}(\mathbf{r}_k)+\sum_{j=1}^{N}T_{kj}\boldsymbol{\mu}_j\right], \tag{2}$$

where $\mathbf{E}(\mathbf{r}_k)$ is the electric field generated by the source dipole $\boldsymbol{\mu}$ on cell k and $T_{kj}=(1/r_{kj}^3)(\delta_{kj}-3\mathbf{r}_{kj}\mathbf{r}_{kj}/r_{kj}^2)$ is the dipole-dipole interaction tensor between cells at positions $\mathbf{r}_k$ and $\mathbf{r}_j$ ($\mathbf{r}_{kj}=\mathbf{r}_k-\mathbf{r}_j$). From the total transition dipole moment thus obtained [Eq. (1)], the lifetime is estimated as (in adimensional units)[28]

$$\tau=\frac{|\boldsymbol{\mu}|^2}{|\boldsymbol{\mu}_{\mathrm{tot}}|^2}. \tag{3}$$

(iii) To build a statistical distribution of the fluorescence lifetimes of a BODIPY molecule embedded in an OS matrix, Monte Carlo realizations of the molecule surrounded by styrene units and holes have been achieved. A Monte Carlo run was implemented in the following way: (1) The fraction of holes (threshold value) was first fixed. (2) For each cell on the lattice, a uniformly distributed (between 0 and 1) random number was chosen. (3) If the random number falls below the threshold value, then the given cell is occupied by a hole, else it is occupied by a monomer. The Monte Carlo simulations were repeated typically 1000 times for each given threshold value.

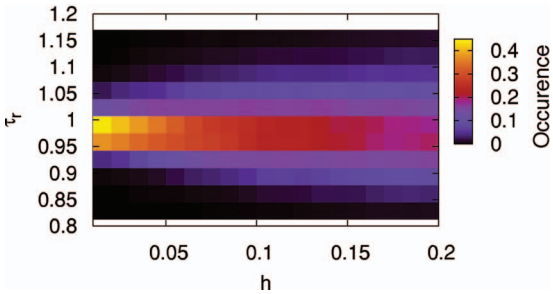

FIG. 7. (Color) Reduced fluorescence lifetime τ_r distributions of a probe as a function of the fraction of holes h introduced in the matrix, calculated by means of Monte Carlo simulations of the system (see text for details).

Figure 7 shows the results of these Monte Carlo simulations for a hole fraction ranging from $h=1\%$ to $h=20\%$ by step of 1%. The distribution of the normalized (with respect to the mean value) fluorescence lifetimes τ_r is very narrow and symmetric around 1 for $h=1\%$. It gets broader and more asymmetric (longer tail) as the fraction of holes is increased.[28,29]

E. Fluorescence lifetime fluctuations: Distributions of holes

On the experimental side, we have estimated the accuracy in the fluorescence lifetime determination by recording a trace of an ensemble of molecules dropped onto a glass substrate from a toluene solution at a probe molecule concentration of $10^{-6}M$, in the same emission conditions (i.e., same emission intensity in the confocal microscope) as the ones applied for the single molecule experiments performed in this study. We have performed the analysis of the recorded trace with the same binning time of the photons (100 ms) as the one chosen in the single molecule experiments in order to get a fair comparison. Figure 8(a) shows the intensity and fluorescence lifetime trajectories of this measurement. The figure clearly shows that for a fluorescence intensity slightly increasing from 10 000 to almost 15 000 counts/s (probably due to solvent evaporation), the value of the determined fluorescence lifetime $\tau=3.44$ ns barely changes. This type of experimental checking is important because it has been reported recently[46] that SPCM modules like the one we are using show a strong shift of the instrumental response function (IRF) with a variation of the count rate, which could make experiments with fluctuating signals difficult to be analyzed quantitatively. According to our results, as evidenced by Fig. 8 (top), this effect does not play a role, as we automatically correct for the shift between the IRF and the decay profile of the molecule in the fitting procedure. As a consequence, the distribution of measured lifetimes in this nonfluctuating environment (on this time scale) is very narrow and gives an estimate on the uncertainty in the lifetime determination (5% of the absolute value of the lifetime, i.e., 0.17 ns in our case). Furthermore, the comparison of this

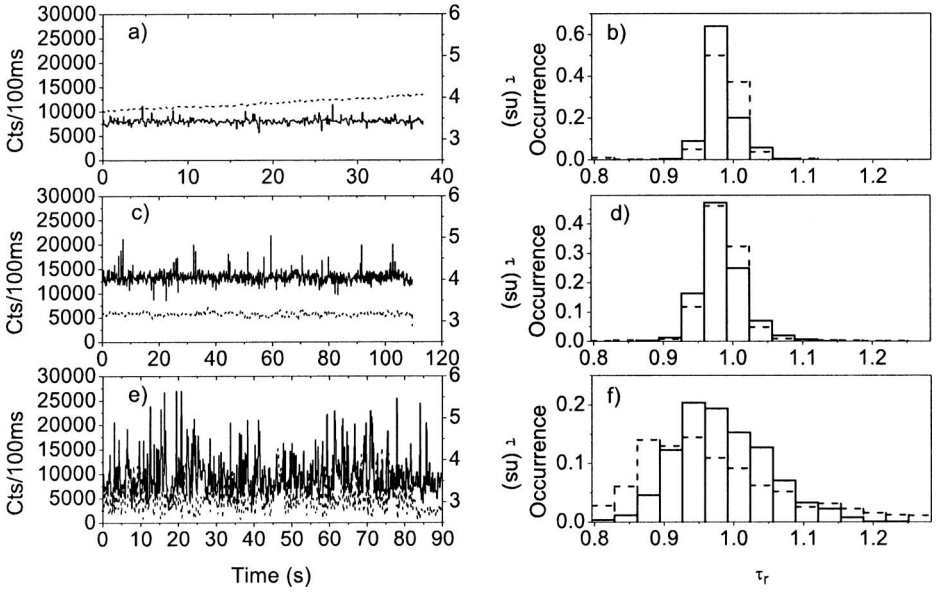

FIG. 8. (Left) (a) Fluorescence intensity (dash) and lifetime (solid) trajectories of dyes embedded in a toluene solution. (c) An OS matrix with M_n =4700 in the glassy state. (e) An OS matrix with M_n=662 and T_g=272 K in the supercooled regime. (Right) Corresponding experimental (dash) lifetime distributions matched with the calculated (solid) ones. The reduced fluorescence lifetime is obtained by dividing the fluorescence lifetime by its average along the trajectory. In the toluene solution (top), the fluctuations of the lifetime can be taken as a measure of the uncertainty in the determination of the lifetime. (b) The corresponding uncertainty in the determination of the fraction of holes is h=1%. (d) h=5%. (f) h=20%.

experimentally obtained distribution with our lifetime simulations also provide a measure for the uncertainty in the determination of the fraction of holes h: Δh=1%.

Figure 8 shows the fluorescence intensity and lifetime trajectories of individual probes embedded in an OS matrix with T_g=322 K [glassy, Fig. 8(c)] and T_g=272 K [supercooled, Fig. 8(e)]. Clearly, the lifetime trajectory displays much more pronounced fluctuations around the mean value in the supercooled regime than in the glassy state. A comparison of the amplitude and frequency of these fluctuations with the (very) small ones exhibited in Fig. 8(a) clearly indicates that the fluctuations only can be the result of different fluctuation dynamics in the different OS matrices. These fluctuations can be accounted for by Monte Carlo simulations of the local density fluctuations,[28] with the fraction of holes surrounding the probe in the matrix as sole parameter. In Figs. 8(d) and 8(f), measured and simulated normalized (with respect to the mean value) radiative lifetime $\tau_r=\tau/\langle\tau\rangle$ histograms are shown for the two OS matrices. In the glassy state, the fraction of holes surrounding the probe is h=5% [Fig. 8(d)], while in the supercooled regime h=20% [Fig. 8(f)].

For the eight polymer matrices of different molecular weights M_n (and hence different T_g values), we recorded the intensity and lifetime trajectories of 50 to 100 single molecules, built the normalized lifetime τ_r distributions, and determined the fraction of holes surrounding each molecule. Figure 9 shows the distributions of the fraction of holes (extracted from the best fits of the MC simulations to the experimental data) as a function of T_g of each investigated matrix. The fraction of holes surrounding the probes peaks in all cases at $h\approx 5\%$ in the glassy state, irrespective of the T_g of the OS sample. A similar h value was found for a different molecular probe (DiD) embedded in a PS matrix,[26] which suggests that this fraction of holes is a characteristic of the polymer in the glassy state. In the supercooled regime ($T > T_g$), the fraction of holes increases up to h=20%. It is worthwhile to note here that for the two matrices explored in the supercooled regime (M_n=662, T_g=272 K and M_n=869, T_g=282 K), 20% of the intensity and lifetime trajectories show a peculiar hopping behavior (not shown) between few levels and were ruled out of the present analysis. This behavior is described elsewhere.[47]

Our results do not agree with the excess free volume concept associated with chain ends: although a reduction of the glass transition temperature is observed by DSC as the degree of polymerization of the chains is decreased, we do not observe an increase of the fraction of holes h in the glassy state. According to the Gibbs and Di Marzio theory, as the temperature is decreased to T_2 at constant pressure, the number of allowed rearrangements for the chains is reduced because (i) the number of holes decreases and the configurational entropy due to permuting holes and chains decreases and (ii) the configurational entropy of the chain decreases because the chains favor low energy states at lower temperatures. At T_2 and lower temperatures, each chain is frustrated by its neighbors and does not reach its Boltzmann equilibrated distribution of shapes. Instead, the distribution encountered at T_2 persists as the temperature is lowered so that the fraction of holes h in the glassy state is constant, as observed. The SMS experimental evidence of a constant fraction of holes below T_2 is furthermore well supported by

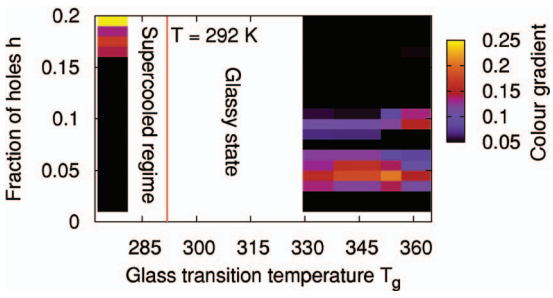

FIG. 9. (Color) Distributions of the fraction of holes surrounding the probe molecules as a function of the glass transition temperature for all samples investigated in this study. A constant fraction of holes h=5% is dominant in the glassy state while h is increased to 20% in the supercooled regime. The working room temperature T=292 K is indicated by the red line.

the parallelism between the volume versus temperature curves for a glass and for a crystal, as evidenced in bulk experiments.

F. Fluorescence lifetime as a function of orientation of the SM with respect to the air interface

In view of the results displayed in Fig. 5 (bottom) [or equivalently Fig. 8(e)] for the fluorescence lifetime of molecule 1 embedded in an OS matrix with M_n=662, i.e., in the supercooled regime for which the matrix allows the SM for having an enhanced mobility, one could argue that the magnitude of the lifetime fluctuations (ratio≈1.6) might be due to reorientations of the SM close to the polymer-air interface. Indeed, the early experiments by Drexhage and Fleck[49] have shown that the spontaneous emission of chromophores close to an interface between two media is altered due to reflection and absorption at the interface. Chance *et al.*[50] and Lukosz and Kunz[51] have described this interaction, showing that the field of the dipole is perturbed by the presence of a second medium. In a simple approximation, a dye molecule can be considered as an oscillating dipole, when driven by the alternating electric field of the incoming light wave. The dipole generates a secondary wave. When surrounded by an isotropic medium, this secondary wave does not influence the oscillator. Close to an interface, the interference with the first and successive reflections of the emitted light wave occurs causing the total radiated power to be strongly dependent on the distance d separating the dipole from the interface, as well as on the orientation α of the dipole with respect to the normal at the interface. This approach, applied in the case of a SM close to an interface, has been well developed in the literature.[52,53]

In order to investigate the influence of the electromagnetic boundary (EB) conditions, due to the presence of the interface, on the fluorescence lifetime of the SM, we follow here a strategy we developed in Ref. 53: We model an oligo(styrene) film containing the SM as a three-layer system consisting of the OS layer sandwiched between air and the glass substrate. Knowing the dielectric constants of the three media, ϵ=1, 2.5, and 2.3, respectively, for air, OS, and glass, we determine numerically[53] the fluorescence lifetime of the molecule embedded in the polymer as a function of depth and orientation with respect to the air interface. Specifically, we consider the cases of the SM situated a distance d =1,2,3,… nm away from the air interface, and having an angle ranging from 0 to 90 in steps of 3.

Figure 10 (top) shows a plot of the fluorescence lifetime versus depth and orientation of a SM located in the 10 nm polymer top layer of a 70 nm thick matrix, where the EB effect is the strongest one, with d=0 at the air-polymer interface, and α=0 as the SM transition dipole is normal to the interface. Remarkably, this figure exhibits a fluorescence lifetime of 3.44 ns for a molecule located at a depth of 1 nm from the interface and having its transition dipole in the plane of the sample. The molecule reaches a lifetime at least four-times larger than this (in-plane) value as the molecule has its transition dipole normal to the plane of the sample. The figure further shows that this effect is reduced as the

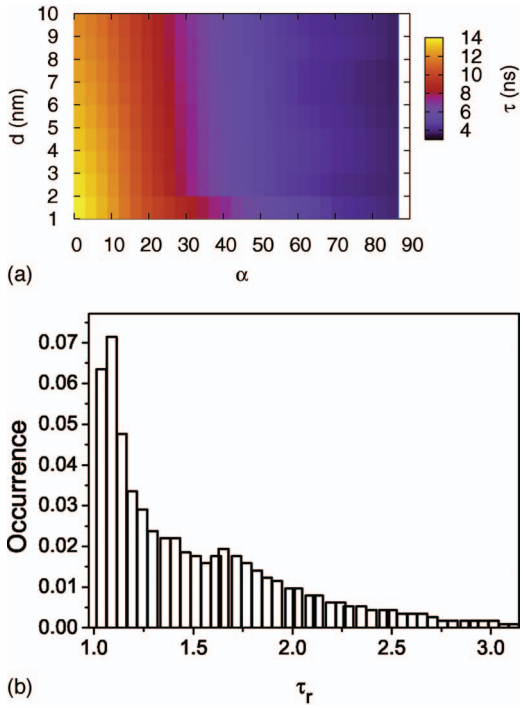

FIG. 10. (Color) (Top) Fluorescence lifetime as a function of orientation α and distance d of the SM with respect to the air interface. We consider here a 70 nm thick film and the SM is in the 10 nm top layer. (Bottom) Reduced fluorescence lifetime τ_r distribution of a SM rotationally and translationally diffusing freely in the 70 nm thick film.

distance between the SM and the interface is increased. So, with no doubt, large changes observed in the fluorescence lifetime of a SM could be attributed to this effect. However, two points have to be considered in order to go further with this possibility: (i) Molecules that are oriented out of plane with respect to the interface are hardly excited by the incoming light beam. Indeed, contrary to 3D techniques[18–22] that aim to enhance the z component of the incoming electric field, usual focusing techniques are used in this study, with a very weak z component of the excitation light. If very large lifetimes are going to be observed, the corresponding intensities of the SM at these times or positions must be very weak. Accordingly, only dipoles with an angle α>30 have a chance to be considered, giving a maximum observable lifetime of ≈9.5 ns. (ii) Molecules show such large variations in the fluorescence lifetime only if they are very close to the interface. Further away, the ratio between out-of-plane and in-plane transition dipoles is strongly reduced.

With these two points in mind, we can exclude the orientational dynamics of the SM close to the polymer-air interface as the cause of the observed lifetime fluctuations. Indeed, only a fraction (typically 10%) of the SMs observed in our study are located close to the air-polymer interface in the more than 100 nm thick polymer film. According to (ii), only this small fraction of the SMs might exhibit the observed lifetime fluctuations. Nevertheless, we observe many more lifetime fluctuating molecules in our study (most of them, in fact). Furthermore, such large lifetimes as 9.5 ns, expected [see (i)] for a SM oriented at α=30 have never been observed. As it is highly improbable that any molecule allowed to rotate close to the interface (previous point)

would not be able to reach this angle, we conjecture that the orientational effect is not the cause of the observed lifetime fluctuations.

In order to strengthen this point, we have simulated the case of a SM allowed to rotationally and translationally diffuse in a 70 nm thick matrix, forcing the angle $\alpha > 30$ (i). We have calculated the fluorescence lifetimes of this SM and built the corresponding distribution. Figure 10 (bottom) shows this fluorescence lifetime distribution. Very interestingly, and as noted previously, the fluorescence lifetimes can be very large, even larger to what we have ever observed. Furthermore, and more importantly, the shape of this distribution does not match the one shown in Fig. 8(f). Specifically, the distribution shown in Fig. 10 (bottom) lacks the lower part (the raising part) of the lifetime distribution shown in Fig. 8(f). The lowest lifetime of a SM close to the interface occurs as the transition dipole moment of this SM is in the plane of the matrix. It can only get larger as the dipole moment is going out of plane, hence the lack of the lower part in Fig. 10 (bottom). The lower part of the distribution shown in Fig. 8(f) results, in fact, from the presence of a void located close to the SM and transversally with respect to the transition dipole axis; the long tail (right part) of this distribution results from the presence of a void located close to the SM and longitudinally with respect to the transition dipole axis.[28] Note that the effect leading to the change in fluorescence lifetime is basically the same if one adopts either the point of view of the electromagnetic boundary conditions[53] or the point of view of a locally fluctuating environment: in both cases, the molecule sees a change in the polarizabilities (or in the high frequency dielectric constant) of its direct surrounding, a molecule oriented out of plane with respect to the air-polymer interface facing basically a big void. However, the in-depth comparison of these approaches allows us to distinguish which mechanism is responsible for the observed lifetime changes. The EB effect associated with the assumption of dynamically reorienting SMs close to the air-polymer interface does not allow one to observe the lower part of the lifetime distribution experimentally observed in Fig. 8(f). Furthermore, the especially long lifetimes expected for significantly out-of-plane oriented molecules have not been observed. On the contrary, the distributions obtained by simulations of a locally fluctuating environment around the SM match very well the experimentally obtained distributions.

IV. CONCLUSIONS

We have shown that the radiative lifetime of single molecules embedded in oligo(styrene) matrices shows large fluctuations induced by the local dielectric environment probed by the dye. This behavior can be reproduced quantitatively by a microscopic version of local field theory when accounting for the presence of holes surrounding the probe molecule. According to these results, two regimes can be clearly distinguished: (i) In the glassy state, the local fraction of holes has been found to be independent of the molecular weight of the polymer and amounts to 5% in the matrices studied here. (ii) The fraction of holes is much larger (close to 20%) once the system is brought in the supercooled regime. These results have been discussed in the framework of the free volume and Gibbs–Di Marzio entropy theories and tend to support the latter, especially in the case of short polymer chains. It is important to keep in mind, however, that the microscopic model used here involves lattice sites of the size of a monomer unit. Hence, fluctuations taking place over more confined spatial domains are not accounted for. While this will not affect the whole picture, such a refinement in the model might improve the agreement between simulated and measured results. Namely, one can notice that the simulated distribution in Fig. 8(f) does not perfectly match the experimental one, with the latter being more asymmetric (as observed in many cases for a molecule in the supercooled regime). This discrepancy is not observed for molecules in the glassy state [Fig. 8(c)]. A more detailed model taking into account a distribution of hole sizes might therefore allow for a more quantitative description of the lifetime fluctuations in the supercooled regime and is currently under scrutiny.

ACKNOWLEDGMENTS

Pascal Damman and Sylvain Desprez (University of Mons, Belgium) are kindly acknowledged for having performed the DSC measurements. The authors thank the Research Fund of the KU Leuven for financial support through GOA2001/2 and GOA2006/2, ZWAP 4/07, and the Belgium Science Policy through IAP 5/03. The Fonds voor Wetenschappelijk Onderzoek Vlaanderen is thanked for a postdoctoral fellowship for one of the authors (R.A.L.V.) and for Grant Nos. G.0320.00 and G.0421.03. Another author (D.B.) is a research associate of the Fonds National de la Recherche Scientifique.

[1] J. Jäckle, Rep. Prog. Phys. **49**, 171 (1986).
[2] W. Götze and L. Sjögren, Rep. Prog. Phys. **55**, 241 (1992).
[3] P. G. Debenedetti, *Metastable Liquids* (Princeton University Press, Princeton, 1997).
[4] E.-W. Donth, *The Glass Transition: Relaxation Dynamics in Liquids and Disordered Materials* (Springer, Berlin, 2001).
[5] *Proceedings of the Fourth International Discussion Meeting on Relaxations in Complex Systems*, edited by K. L. Ngai, special issues of J. Non-Cryst. Solids 307–310 (2002).
[6] K. Binder and W. Kob, *Glassy Materials and Disordered Solids: An Introduction to their Statistical Mechanics* (World Scientific, Singapore, 2005).
[7] H. Sillescu, J. Non-Cryst. Solids **243**, 81 (1999).
[8] M. D. Ediger, Annu. Rev. Phys. Chem. **51**, 99 (2000).
[9] R. Richert, J. Phys.: Condens. Matter **24**, R703 (2002).
[10] W. E. Moerner and M. Orrit, Science **283**, 1670 (1999).
[11] X. S. Xie and J. K. Trautman, Annu. Rev. Phys. Chem. **49**, 441 (1998).
[12] F. Kulzer and M. Orrit, Annu. Rev. Phys. Chem. **55**, 585 (2004).
[13] R. A. L. Vallée, M. Cotlet, J. Hofkens, F. C. De Schryver, and K. Müllen, Macromolecules **36**, 7752 (2003).
[14] L. A. Deschenes and D. A. Vanden Bout, J. Phys. Chem. B **106**, 11438 (2002).
[15] N. Tomczak, R. A. L. Vallée, E. M. H. P. van Dijk, M. García-Parajó, L. Kuipers, N. F. van Hulst, and G. J. Vancso, Eur. Polym. J. **40**, 1001 (2004).
[16] A. Schob, F. Cichos, J. Schuster, and C. von Borczyskowski, Eur. Polym. J. **40**, 1019 (2004).
[17] E. Mei, J. Tang, J. M. Vanderkooi, and R. M. Hochstrasser, J. Am. Chem. Soc. **125**, 2730 (2003).
[18] R. M. Dickson, D. J. Norris, and W. E. Moerner, Phys. Rev. Lett. **81**, 5322 (1998).
[19] B. Sick, B. Hecht, and L. Novotny, Phys. Rev. Lett. **85**, 4482 (2000).

[20] A. Lieb, J. M. Zavislan, and L. Novotny, J. Opt. Soc. Am. B **21**, 1210 (2004).
[21] M. Böhmer and J. Enderlein, J. Opt. Soc. Am. B **20**, 554 (2000).
[22] H. Uji-i, S. Melnikov, A. Deres, G. Bergamini, F. De Schryver, A. Herrmann, K. Müllen, J. Enderlein, and J. Hofkens, Polymer **47**, 2511 (2006).
[23] A. P. Bartko, K. Xu, and R. M. Dickson, Phys. Rev. Lett. **89**, 026101 (2002).
[24] R. A. L. Vallée, N. Tomczak, L. Kuipers, G. J. Vancso, and N. F. van Hulst, Phys. Rev. Lett. **91**, 038301 (2003).
[25] R. A. L. Vallée, N. Tomczak, L. Kuipers, G. J. Vancso, and N. F. van Hulst, Chem. Phys. Lett. **384**, 5 (2004).
[26] N. Tomczak, R. A. L. Vallée, E. M. H. P. van Dijk, L. Kuipers, N. F. van Hulst, and G. J. Vancso, J. Am. Chem. Soc. **126**, 4748 (2004).
[27] R. A. L. Vallée, N. Tomczak, G. J. Vancso, L. Kuipers, and N. F. van Hulst, J. Chem. Phys. **122**, 114704 (2005).
[28] R. A. L. Vallée, M. Van der Auweraer, F. C. De Schryver, D. Beljonne, and M. Orrit, ChemPhysChem **6**, 81 (2005).
[29] R. A. L. Vallée, P. Marsal, E. Braeken, S. Habuchi, F. C. De Schryver, M. Van der Auweraer, D. Beljonne, and J. Hofkens, J. Am. Chem. Soc. **127**, 12011 (2005).
[30] T. G. Fox and P. J. Flory, J. Am. Chem. Soc. **70**, 2384 (1948).
[31] G. Pezzin, F. Zilio-Grandi, and P. Sanmartin, Eur. Polym. J. **6**, 1053 (1970).
[32] J. H. Gibbs and E. A. Di Marzio, J. Chem. Phys. **28**, 373 (1958).
[33] M. Maus, M. Cotlet, J. Hofkens, T. Gensch, F. C. De Schryver, J. Schaffer, and C. A. M. Seidel, Anal. Chem. **73**, 2078 (2001).
[34] R. Hanbury-Brown and R. Q. Twiss, Nature (London) **177**, 27 (1956).
[35] M. J. S. Dewar, E. G. Zoebisch, E. F. Healy, and J. J. P. Stewart, J. Am. Chem. Soc. **107**, 3902 (1985).
[36] AMPAC, Semichem, 7204 Mullen, Shawnee, KS 66216.
[37] M. C. Zerner, G. H. Loew, R. Kichner, and U. T. Mueller-Westerhoff, J. Am. Chem. Soc. **122**, 3015 (2000).
[38] T. Basché, W. E. Moerner, M. Orrit, and H. Talon, Phys. Rev. Lett. **69**, 1516 (1992).
[39] L. Fleury, J.-M. Segura, G. Zumofen, B. Hecht, and U. P. Wild, Phys. Rev. Lett. **84**, 1148 (2000).
[40] B. Lounis and W. E. Moerner, Nature (London) **407**, 491 (2000).
[41] P. Tinnefeld, C. Muller, and M. Sauer, Chem. Phys. Lett. **345**, 252 (2001).
[42] P. Tinnefeld, K. D. Weston, T. Vosch, M. Cotlet, T. Weil, J. Hofkens, K. Müllen, F. C. De Schryver, and M. Sauer, J. Am. Chem. Soc. **124**, 14310 (2002).
[43] S. Masuo, T. Vosch, M. Cotlet *et al.*, J. Phys. Chem. B **108**, 16686 (2004).
[44] C.-Y. Lu and D. A. Vanden Bout, J. Chem. Phys. **125**, 124701 (2006).
[45] H. Yang and X. S. Xie, J. Chem. Phys. **117**, 10965 (2002).
[46] S. Felekyan, R. Kühnemuth, V. Kudryavtsev, C. Sandhagen, W. Becker, and C. A. M. Seidel, Rev. Sci. Instrum. **76**, 083104 (2005).
[47] R. A. L. Vallée, M. Van der Auweraer, W. Paul, and K. Binder, Phys. Rev. Lett. **97**, 217801 (2006).
[48] The reason why we observe an increase of the residuals at long time scale ($t > 12$ ns) is unclear. It is probably due to a small contribution of naturally occurring long lifetimes in the time trajectories [Fig. 5 (bottom)]. Nevertheless, we do not succeed to best fit the profile with a multiexponential function.
[49] K. H. Drexhage and M. Fleck, Ber. Bunsenges. Phys. Chem. **72**, 330 (1968).
[50] R. R. Chance, A. Prock, and R. Silbey, Adv. Chem. Phys. **37**, 1 (1978).
[51] W. Lukosz and R. E. Kunz, J. Opt. Soc. Am. **67**, 1607 (1977); T. Basché, Abstr. Pap. - Am. Chem. Soc. **S221**, U235 (2001).
[52] J. J. Macklin, J. K. Trautman, T. D. Harris, and L. E. Brus, Science **272**, 255 (1996).
[53] R. A. L. Vallée, N. Tomczak, H. Gersen, E. M. H. P. van Dijk, M. F. García-Parajó, G. J. Vancso, and N. F. van Hulst, Chem. Phys. Lett. **348**, 161 (2001).